NASA/TM-2008-215331
ARL-TR-4472

Fatigue Crack Growth Threshold Testing of Metallic Rotorcraft Materials

John A. Newman
Langley Research Center, Hampton, Virginia

Mark A. James
Alcoa Technical Center, Pittsburgh, Pennsylvania

William M. Johnston
Lockheed Martin Engineering and Sciences
Langley Research Center, Hampton, Virginia

Dy D. Le
U. S. Army Research Laboratory
Vehicle Technology Directorate
Langley Research Center, Hampton, Virginia

July 2008

The NASA STI Program Office . . . in Profile

Since its founding, NASA has been dedicated to the advancement of aeronautics and space science. The NASA Scientific and Technical Information (STI) Program Office plays a key part in helping NASA maintain this important role.

The NASA STI Program Office is operated by Langley Research Center, the lead center for NASA's scientific and technical information. The NASA STI Program Office provides access to the NASA STI Database, the largest collection of aeronautical and space science STI in the world. The Program Office is also NASA's institutional mechanism for disseminating the results of its research and development activities. These results are published by NASA in the NASA STI Report Series, which includes the following report types:

- TECHNICAL PUBLICATION. Reports of completed research or a major significant phase of research that present the results of NASA programs and include extensive data or theoretical analysis. Includes compilations of significant scientific and technical data and information deemed to be of continuing reference value. NASA counterpart of peer-reviewed formal professional papers, but having less stringent limitations on manuscript length and extent of graphic presentations.

- TECHNICAL MEMORANDUM. Scientific and technical findings that are preliminary or of specialized interest, e.g., quick release reports, working papers, and bibliographies that contain minimal annotation. Does not contain extensive analysis.

- CONTRACTOR REPORT. Scientific and technical findings by NASA-sponsored contractors and grantees.

- CONFERENCE PUBLICATION. Collected papers from scientific and technical conferences, symposia, seminars, or other meetings sponsored or co-sponsored by NASA.

- SPECIAL PUBLICATION. Scientific, technical, or historical information from NASA programs, projects, and missions, often concerned with subjects having substantial public interest.

- TECHNICAL TRANSLATION. English-language translations of foreign scientific and technical material pertinent to NASA's mission.

Specialized services that complement the STI Program Office's diverse offerings include creating custom thesauri, building customized databases, organizing and publishing research results ... even providing videos.

For more information about the NASA STI Program Office, see the following:

- Access the NASA STI Program Home Page at ***http://www.sti.nasa.gov***

- E-mail your question via the Internet to help@sti.nasa.gov

- Fax your question to the NASA STI Help Desk at (301) 621-0134

- Phone the NASA STI Help Desk at (301) 621-0390

- Write to:
  NASA STI Help Desk
  NASA Center for AeroSpace Information
  7115 Standard Drive
  Hanover, MD 21076-1320

NASA/TM-2008-215331
ARL-TR-4472

Fatigue Crack Growth Threshold Testing of Metallic Rotorcraft Materials

John A. Newman
Langley Research Center, Hampton, Virginia

Mark A. James
Alcoa Technical Center, Pittsburgh, Pennsylvania

William M. Johnston
Lockheed Martin Engineering and Sciences
Langley Research Center, Hampton, Virginia

Dy D. Le
U. S. Army Research Laboratory
Vehicle Technology Directorate
Langley Research Center, Hampton, Virginia

National Aeronautics and
Space Administration

Langley Research Center
Hampton, Virginia 23681-2199

July 2008

Available from:

NASA Center for AeroSpace Information (CASI)
7115 Standard Drive
Hanover, MD 21076-1320
(301) 621-0390

National Technical Information Service (NTIS)
5285 Port Royal Road
Springfield, VA 22161-2171
(703) 605-6000

Abstract

Results are presented for a program to determine the near-threshold fatigue crack growth behavior appropriate for metallic rotorcraft alloys. Four alloys, all commonly used in the manufacture of rotorcraft, were selected for study: Aluminum alloy 7050, 4340 steel, AZ91E Magnesium, and Titanium alloy Ti-6Al-4V (β-STOA). The Federal Aviation Administration (FAA) sponsored this research to advance efforts to incorporate damage tolerance design and analysis as requirements for rotorcraft certification. Rotocraft components are subjected to high-cycle fatigue and are typically subjected to higher stresses and more stress cycles per flight hour than fixed-wing aircraft components. Fatigue lives of rotorcraft components are generally spent initiating small fatigue cracks that propagate slowly under near-threshold crack-tip loading conditions. For these components, the fatigue life is very sensitive to the near-threshold characteristics of the material.

Introduction

Up to the 1990s, rotorcraft have been designed almost exclusively using the safe-life philosophy with the Palmgren and Miner rule of linear cumulative damage being used to establish retirement times for the dynamic components (refs. 1,2). Safe-life has been a fairly reliable design approach for rotorcraft. However, the safe-life approach has a number of critical limitations: it does not include a way to quantify reliability; it increases maintenance costs because it requires parts be retired even if they have no detectable damage; and most importantly, it does not model cracks, the predominant root cause of structural failure. These limitations and others have led the Federal Aviation Administration (FAA) to consider implementing the damage tolerance (DT) design approach into the federal air regulations (FAR). One study in the 1980s (ref. 3) showed that some rotorcraft components in a safe-life designed rotorcraft could be managed using DT while others would have to be redesigned. A more recent analytical study (ref. 4) showed how important the crack-growth threshold values were on determining adequate inspection intervals. Due to the high-cycle load content of rotorcraft load spectra, approximately 12,000 cycles per hour compared to 120 cycles per hour for a fighter aircraft, once loads exceed the crack growth threshold very short crack-growth lives often exist.

The crack-growth rate threshold, ΔK_{th}, shown in Figure 1 is the value of the stress intensity below which cracks propagate at an insignificant rate. Most of the data in the literature for ΔK_{th} is obtained through a test procedure called the constant R load reduction procedure, where R is called the stress ratio, $R = S_{min} / S_{max} = K_{min} / K_{max}$. In the constant R load reduction procedure, the cyclic load is continually decreased during the test. This causes the crack driving force, ΔK, to diminish until the crack growth rate is at or below a sufficiently low value, typically 3.9×10^{-9} inch/cycle (10^{-10} m/cycle) per the American Society for Testing and Materials (ASTM) standard E647 (ref. 5). During the last decade, some studies have suggested that non-conservative values for the threshold can be generated using this procedure (refs. 6, 7). Other studies have shown that the constant-R load reduction procedure may produce threshold values only about 10% higher than detailed compression precracking procedures designed to avoid load history effects, here, defined as crack growth rate data that varies due to test loading history (refs. 6, 8, 9). For high-cycle-fatigue applications, like many rotorcraft components, it is important to accurately determine the crack growth threshold. Non-conservative values (estimated too low) may result in premature structural failure while overly conservative values (estimated too high) may degrade rotorcraft performance due to excessive structural weight.

The original objective of this project was aimed at avoiding load history effects using a procedure where compression precracking followed by increasing load is used as an alternate procedure for generating fatigue crack-growth rate threshold data. This compression precracking (CPC) procedure, as originally proposed, would produce the entire d*a*/dN-versus-ΔK curve from threshold to failure in a single increasing-ΔK test. However, recent analytical and experimental results of the CPC test procedure has shown that load history effects exist even in this test procedure. Specifically, finite element results have shown that a tensile residual stress field exists as a result of the compression loading, and is supported with experimental results (ref. 10). Modifications to the CPC test procedure have been proposed in an effort to eliminate residual stress effects, but, at this time, no such method has proven successful (ref. 10). Detailed examples of CPC test results are provided in the Appendix.

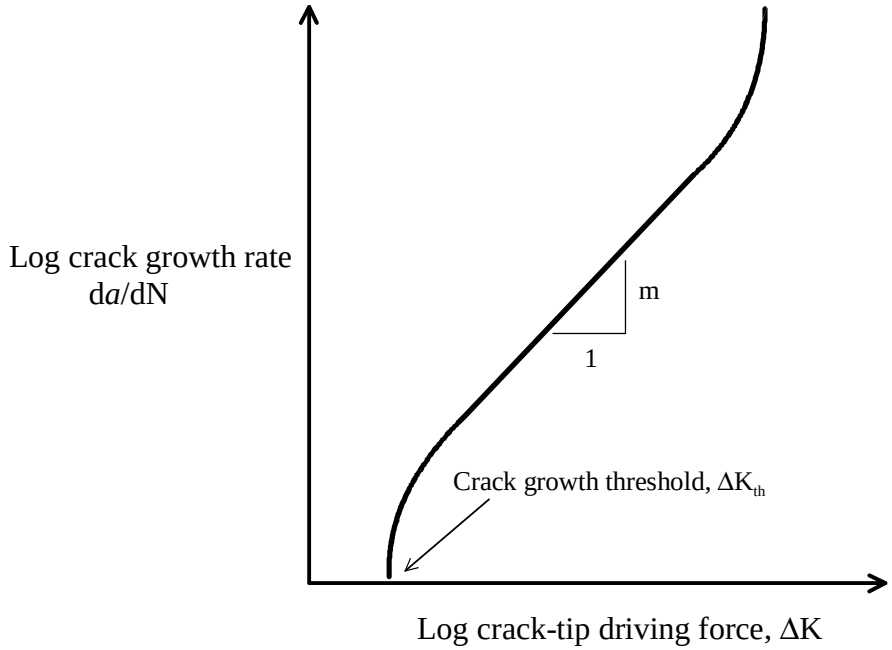

Figure 1. Schematic of typical fatigue crack-growth rate data.

After learning of the CPC testing issues, the project was refocused to better provide technical support to the rotorcraft industries to allow helicopter components to be designed and managed using damage-tolerance fatigue life methods. As previously stated, some research results suggest that the current ASTM-standard fatigue crack growth (FCG) test method, ASTM E647 (ref. 5), may produce non-conservative results under certain conditions (ref. 11). However, the effect of load history on test data is uncertain because some research results indicate that the current test method is only affected by load history for certain conditions. Load history effects represent a potential shortcoming with the standard test method and are a major technical issue that must be addressed because the fatigue lives of most rotorcraft components are dominated by the near-threshold FCG behavior.

The rotorcraft program is a continuation of a similar program for propeller materials (ref. 12). One of the broad objectives of that program was to develop and validate the original CPC concept. In conjunction with that program, and as a result of unexpected experimental results, finite element analyses were run to explore the possible effects of residual stresses on crack growth rate data. Analysis results, as well as subsequent testing on 7050 aluminum sheet material, showed that for the loading levels investigated, the residual stresses caused by the compression precracking affected the crack growth rate data until the crack grew approximately 2-3 times the estimated compression-induced notch-tip plastic

zone (ref. 10). The loading levels investigated were somewhat above the fatigue crack growth threshold (ΔK_{th} = 3 ksi$\sqrt{in}$ is typical of 7000-series aluminum alloys). The effects may be slightly larger for lower loading levels and slightly lower at higher loading levels. These analytical and experimental results have challenged the validity of the original CPC test method and influenced the direction of this program.

The first objective of the re-focused test plan is to examine the potential problems with the standard FCG test method and, if needed, propose alternate test methods to obtain near-threshold FCG data that is not affected by load history. Both experimental and analytical methods may be used to achieve this objective. The second objective of this project is to perform tests on materials commonly used in rotorcraft so that the experimental results can be directly used by the rotorcraft industries. This proposed work would compliment the propeller research to verify and modify the CPC test method to eliminate residual stress effects. Because these alternate plans involve some ΔK-reduction tasks, and some research results suggest that any ΔK-reduction scheme would result in load-history-induced closure (refs. 9, 10), it is even more important to evaluate the effect of the ΔK-reduction test method. Finally, if guidelines on acceptable load history can be established that are useful for evaluating the wealth of current data in the literature and in industry databases, retesting all potentially affected materials may be avoided.

Materials

Four materials were selected for study: aluminum alloy 7050, 4340 steel, AZ91E magnesium, and Ti-6Al-4V (β-STOA). Two of these materials are well-behaved and ideal for evaluating load history effects; aluminum alloy 7050 and 4340 steel. The two remaining materials (AZ91E magnesium and Ti-6Al-4V) can be investigated using the standard method (ASTM E647) at the most critical stress ratio for load history effects (R = 0.1) and using the constant-K_{max} procedure to obtain closure-free data. While Ti-6Al-4V (β-STOA) is a critical and valuable alloy for industry, the same characteristics that make it highly desirable also make it a potentially difficult alloy to use for evaluating load history effects. Specifically, this alloy has been provided in a forged product form with an unknown residual stress state, and has an extremely course microstructure (grain diameter of approximately 1 mm or 1,000 microns) that is likely to result in crack branching and high crack closure levels due to crack-wake roughness. The magnesium alloy, provided in the form of cast plates, is likely better behaved, but has low fracture toughness (K_{Ic} < 15 ksi$\sqrt{in}$) and fatigue crack growth threshold (ΔK_{th}) values.

Fatigue Crack Growth Threshold Testing

To evaluate the current test method, it is proposed that a series of standard ΔK-reduction tests be performed, each with a different load history by choosing a different initial ΔK value or K-gradient. Substantial evidence from the literature shows that high starting ΔK values can result in load history effects, but no detailed study has been performed (ref. 13). This same study showed that different specimen configurations (K_b surface crack and through-thickness compact tension (CT) specimens) give the same FCG threshold if starting test conditions are carefully controlled. The CT specimen size in reference 12 is smaller (width, W = 2 inches) than that used by the previously funded FAA propeller program (W = 3 inches). This rotorcraft program uses both CT specimen configurations (width, W = 2 inches and thickness, B = 0.25 inches for 7050 aluminum and AZ91E magnesium; W = 3 and B = 0.5 inches for 4340 steel and Ti-6Al-4V). Tests with different starting ΔK values (ΔK_i) that produce the same fatigue crack growth rate data are assumed to be unaffected by load history. As an example, consider three sets of crack growth data, all identical with the exception of the initial ΔK value. If the data for the low and intermediate initial ΔK values coincide, but the data for the high initial ΔK value differs (see Figure 2a), then it is assumed that tests started at or below the intermediate ΔK value will be free of load

history effects. If all three data sets were to coincide (see Figure 2b), then there would be no evidence of load history effects.

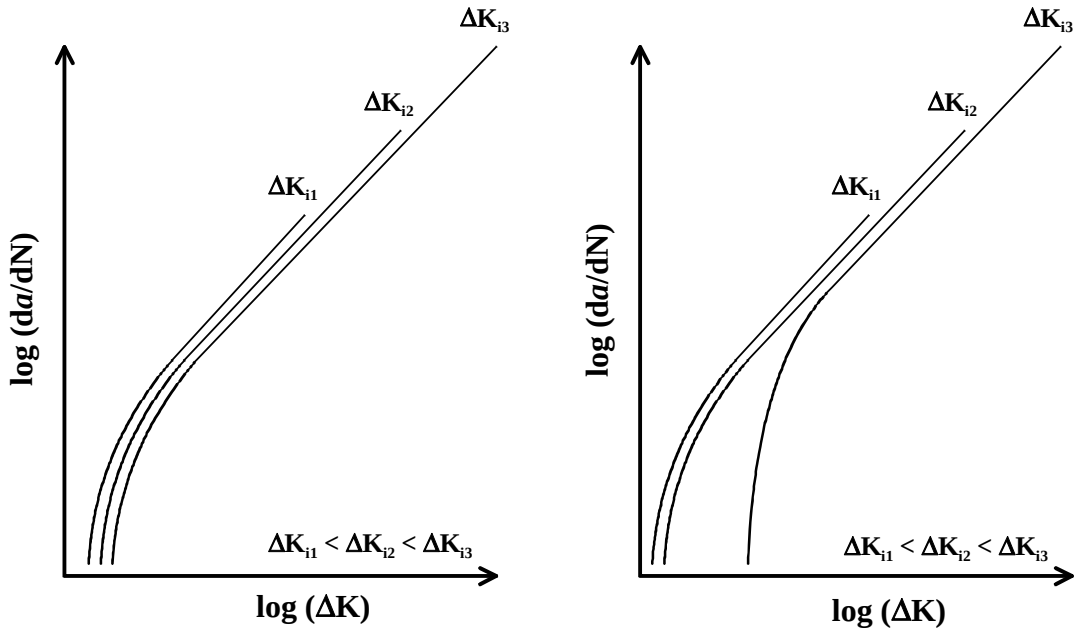

(a) Affected by load history (b) Not affected by load history

Figure 2. Schematics of expected crack growth behavior for ΔK-reduction testing.

Experimental Results

Aluminum Alloy 7050

CT specimens (W = 2 inches and B = 0.25 inches) were machined from 6-inch-thick plate material in the L-T orientation.[1] During testing, crack length was monitored using back face compliance data, and loads were continuously adjusted to achieve programmed stress intensity factors. A series of tests were conducted using constant-R and constant-K_{max} test methods outlined in ASTM standard E647 (ref. 5). Tests were conducted such that ΔK was smoothly and gradually changed with increasing crack length. The rate of change in ΔK is defined by the K-gradient, C. For constant-R decreasing-ΔK tests, a K-gradient of C = -2/inch was used, while C = -10/inch was used during constant-K_{max} decreasing-ΔK tests. Multiple constant-R tests were conducted for three different values of R (0.1, 0.5, and 0.7). Initial loads were varied to alter the likelihood of load history effects; tests started at higher ΔK values would be more likely affected by load history due to higher plasticity levels at the start of the test.

Constant-R = 0.1 test data are shown in Figure 3 to highlight differences in crack growth rates due to starting ΔK values. Here four tests are shown, each with a different initial ΔK value. The standard test procedure (ASTM E647) suggests that constant-R ΔK-decreasing tests be started at crack growth rates no greater than $4x10^{-7}$ inch/cycle (10^{-8} m/cycle). However, for this study, this guideline is violated to characterize the effect of initial ΔK, ΔK_i. The data for the highest initial ΔK (ΔK_i = 9 ksi√in) show a crack growth threshold of approximately ΔK_{th} = 2.6 ksi√in, which is slightly lower than the threshold

[1] For crack growth specimens made from rolled sheet or plate product forms, the L-T orientation means that the axis of loading corresponds to the longitudinal (L) direction and crack growth is in the long-transverse (T) direction.

value for ΔK_i = 7.2 ksi√in (ΔK_{th} = 2.7 ksi√in). Results for the lowest initial ΔK (ΔK_i = 3.1 ksi√in) produced a threshold of approximately ΔK_{th} = 2.45 ksi√in, which is slightly higher than the result for ΔK_i = 4.5 ksi√in (ΔK_{th} = 2.2 ksi√in).

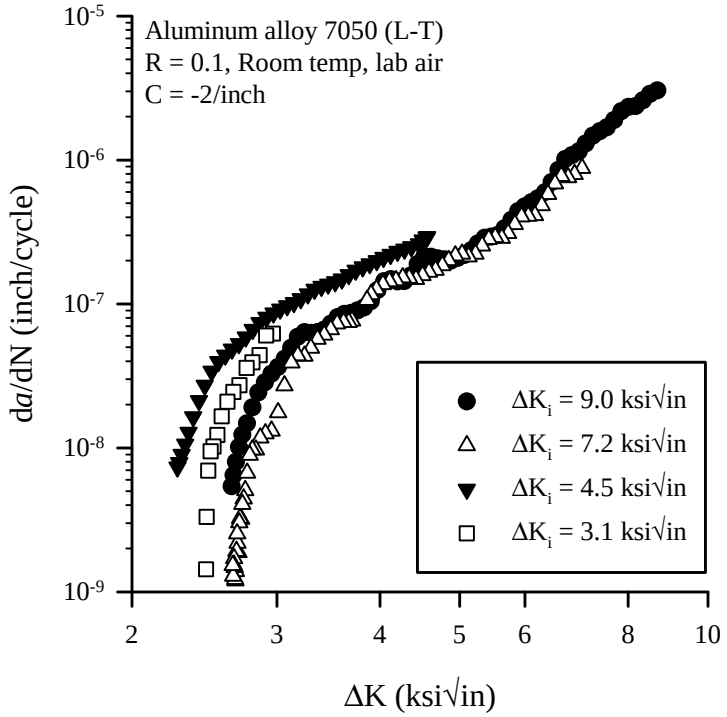

Figure 3. Constant-R = 0.1 fatigue crack growth data for aluminum alloy 7050.

Examination of the near-threshold data in Figure 3 (for example, at d*a*/dN = 10^{-8} inch/cycle) reveals that the near threshold crack growth rates for tests started at the extremely high and low initial ΔK values are bounded by the test data started at the intermediate initial ΔK values.[2] Were the variations in ΔK_{th} for these tests a result of load history, ΔK_{th} values corresponding to high initial ΔK tests would be expected to be higher than those for low initial ΔK tests. The variations in ΔK_{th} for the data in Figure 3 (2.2 ksi√in < ΔK_{th} < 2.7 ksi√in) appear to be somewhat independent of the load history. This observation suggests that something else may be affecting these data, e.g., environmental variables such as humidity.

Constant-R = 0.5 test data for 7050 aluminum are shown in Figure 4 for initial ΔK values of ΔK_i = 2.5 ksi√in and 5.0 ksi√in. The crack growth thresholds for these tests are approximately ΔK_{th} = 1.55 ksi√in and 1.65 ksi√in, respectively. These data suggest that a subtle load history effect may exist, although, this small difference in ΔK_{th} may be explained by other factors, e.g., environment. Further testing, beyond the scope of this study, is needed to settle this issue.

Constant-R = 0.7 test data for 7050 aluminum are shown in Figure 5 both increasing and decreasing ΔK tests. All data are in excellent agreement suggesting that the crack growth rate data are not affected by differences in load history. These results indicate that the crack growth threshold for R = 0.7 is approximately ΔK_{th} = 1.4 ksi√in, and seems to be independent of load history for ΔK_i < 5 ksi√in.

[2] Axes on the plots presented in this paper are scaled to best observe differences between similar sets of data. Although no effort is made to maintain consistency in scaling of axes, no attempt is made in this paper to compare results for different materials or load ratio shown in other plots.

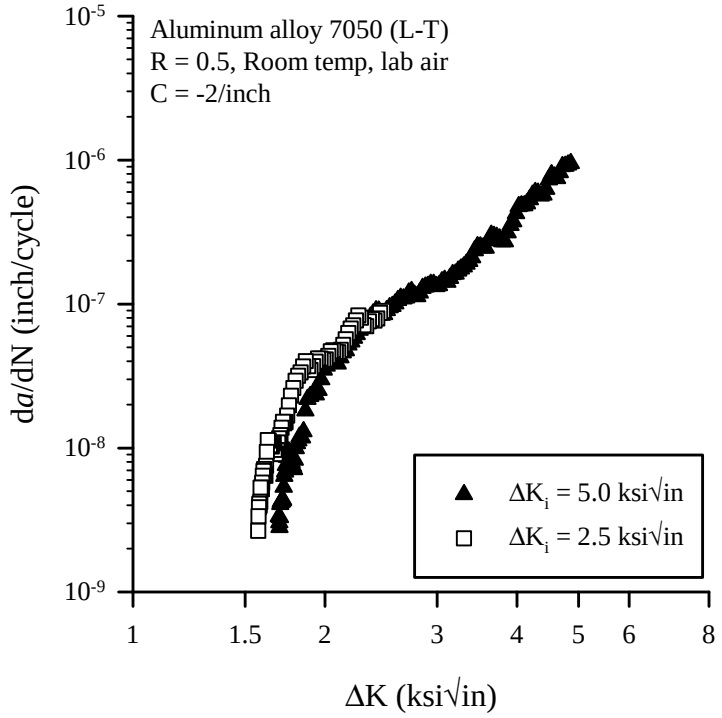

Figure 4. Constant-R = 0.5 fatigue crack growth data for aluminum alloy 7050.

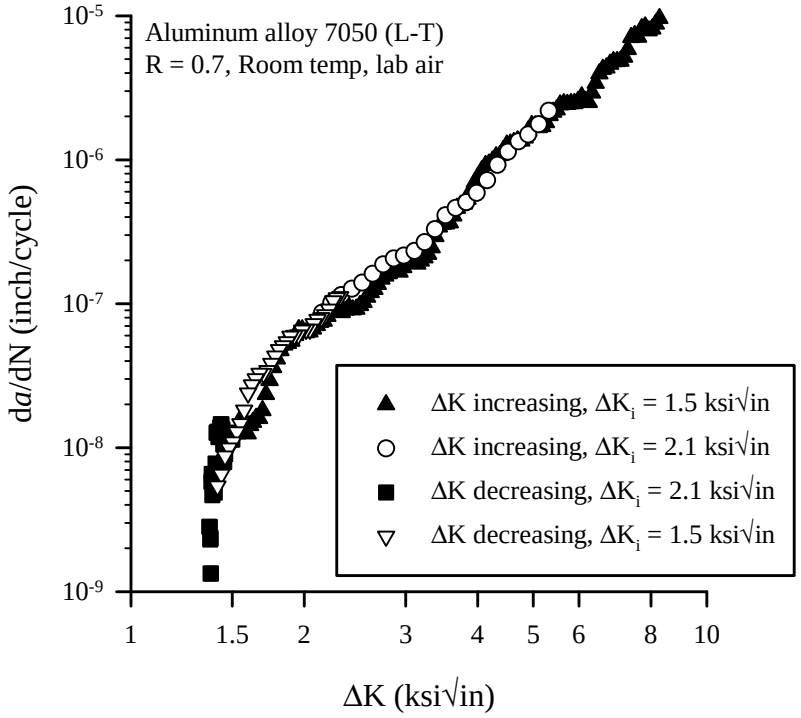

Figure 5. Constant-R = 0.7 fatigue crack growth data for aluminum alloy 7050.

Constant-K_{max} test data for 7050 aluminum are shown in Figure 6 for K_{max} values of 5 ksi√in, 10 ksi√in, and 15 ksi√in. In general, the near-threshold crack growth data for higher K_{max} values are slightly greater than the corresponding rates for tests at lower K_{max} values. However, these differences appear to be small, and result in threshold values ranging from ΔK_{th} = 1.25 ksi√in to ΔK_{th} = 1.15 ksi√in. The subtle decrease in ΔK_{th} with increasing K_{max} value observed in Figure 6 is similar to that observed in other commonly-used 7000-series aluminum alloys (ref. 14). The deviation observed in the K_{max} = 5 ksi√in data for ΔK > 3 ksi√in (R < 0.4) is a result of crack closure that occurs at low values of R near the start of constant-K_{max} tests.

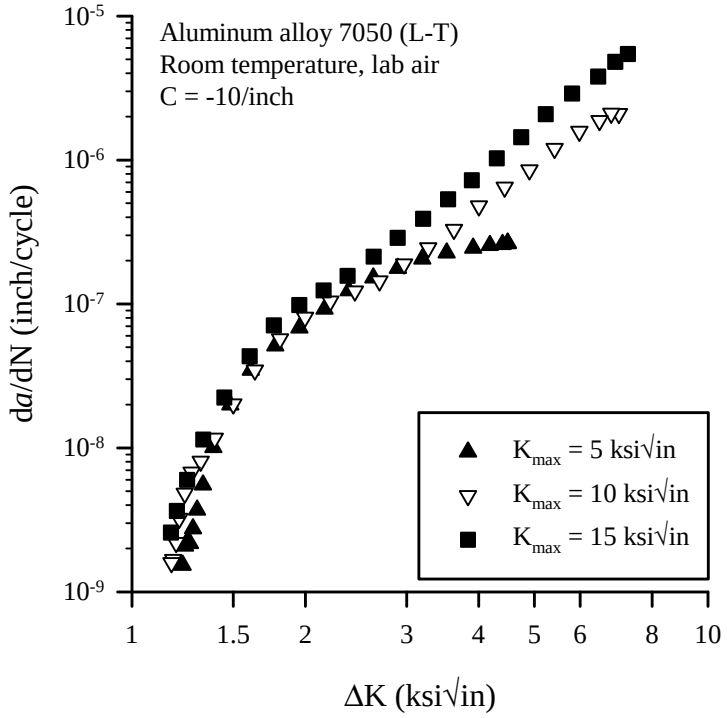

Figure 6. Constant-K_{max} fatigue crack growth data for aluminum alloy 7050.

4340 Steel

The compact tension specimens used in this study (W = 3 inches, B = 0.5 inches) were machined from 4340 steel forgings. Fatigue crack growth tests were performed in computer-controlled servo-hydraulic machines. Fatigue tests on this alloy, for a similar study on propeller materials, showed little evidence of load history effects (ref. 12).

Constant-R = 0.1 fatigue crack growth test data for 4340 steel are plotted in Figure 7. Data are shown for increasing-ΔK (C = +5/inch) and decreasing-ΔK (C = -2/inch) conditions. Based on these data, the fatigue crack growth threshold is approximately ΔK_{th} = 8.0 ksi√in. Note that this value of crack growth threshold is slightly higher than that value reported in reference 12 (ΔK_{th} = 7 ksi√in), however, this difference is likely due to the differences in product forms and processing of different manufacturers. The excellent agreement between all three sets of data suggests an absence of load history effects.

Fatigue crack growth data for R = 0.3 and 0.7 are plotted in Figures 8 and 9, respectively, for multiple tests performed with a variety of load histories (ΔK-increasing and ΔK-decreasing). For the R = 0.3 test

condition, the fatigue crack growth threshold is approximately ΔK_{th} = 5.8 ksi√in, while the threshold value corresponding to the R = 0.7 condition is nearly ΔK_{th} = 3.0 ksi√in. Although, reference 12 does not provide any R = 0.3 test data for comparison, the crack growth results for R = 0.7 are in excellent agreement with the results of Figure 9. For each load ratio, the excellent agreement between all data sets, regardless of difference in load history, suggests that load history effects are negligible.

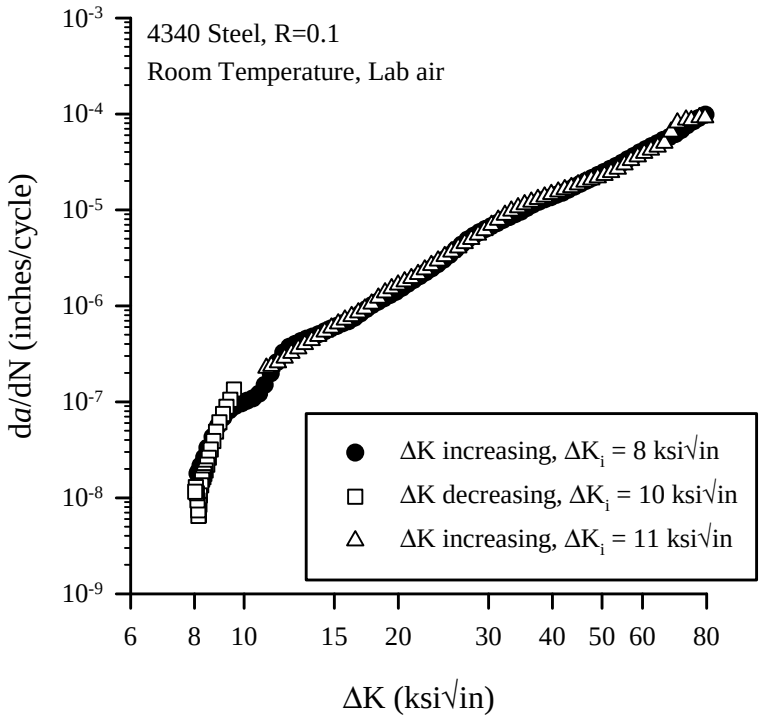

Figure 7. Constant-R = 0.1 fatigue crack growth data for 4340 steel.

Constant-K_{max} fatigue crack growth data are plotted in Figure 10 for three different values of K_{max} (K_{max} = 11 ksi√in, 15 ksi√in, and 30 ksi√in). The near-threshold results (ΔK < 5 ksi√in) for all three sets of data are in good agreement, as expected for commonly used engineering alloys where the majority of load ratio effects are a result of crack closure. Since crack closure is less important at high-R conditions the value of fatigue crack growth threshold, here approximately ΔK_{th} = 2.8 ksi√in is very nearly equal to the result for R = 0.7 (recall Figure 9, ΔK_{th} = 3.0 ksi√in).

Ti-6-4 β-STOA

A titanium alloy (Ti-6Al-4V) was provided by a rotorcraft manufacturer in forgings of the β-STOA (solution treated over aged) condition. As provided, this alloy has a very coarse microstructure having nearly equi-axed grains nearly 1 mm (0.04 inches) in diameter. Compact tension specimens (W = 3 inches, B = 0.5 inches) were machined from near-net-shape forgings. Larger specimens were used for this material due to the coarse microstructure.

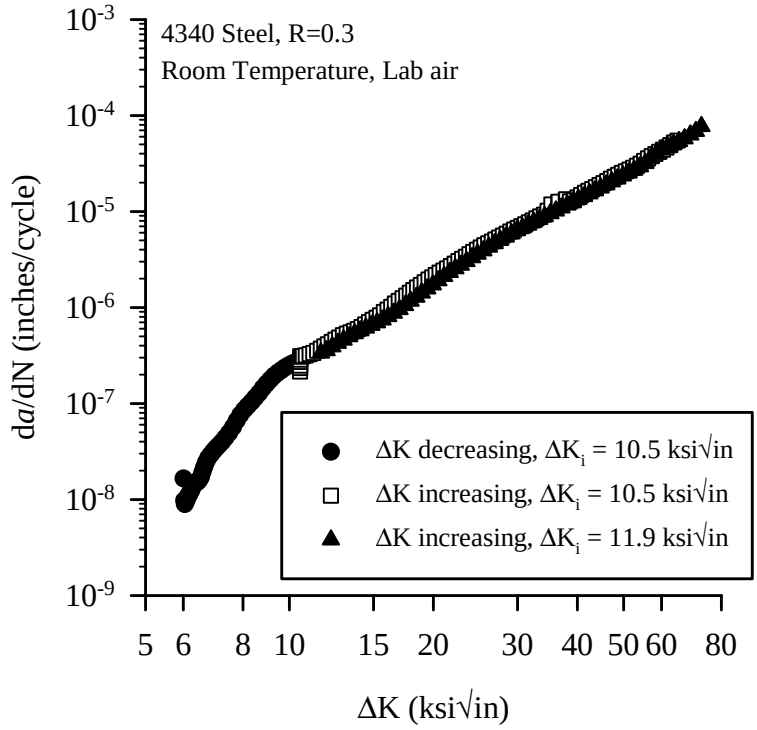

Figure 8. Constant-R = 0.3 fatigue crack growth data for 4340 steel.

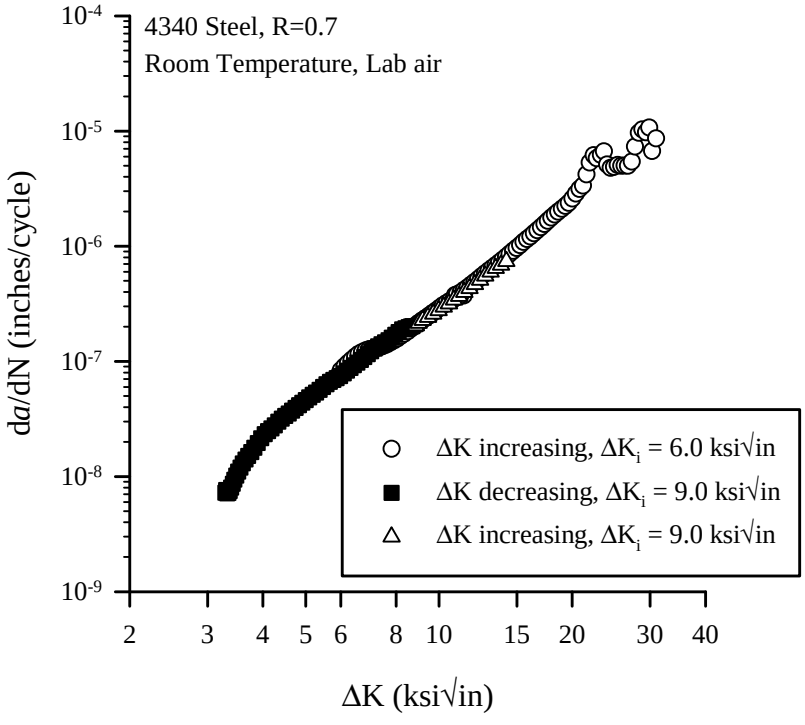

Figure 9. Constant-R = 0.7 fatigue crack growth data for 4340 steel.

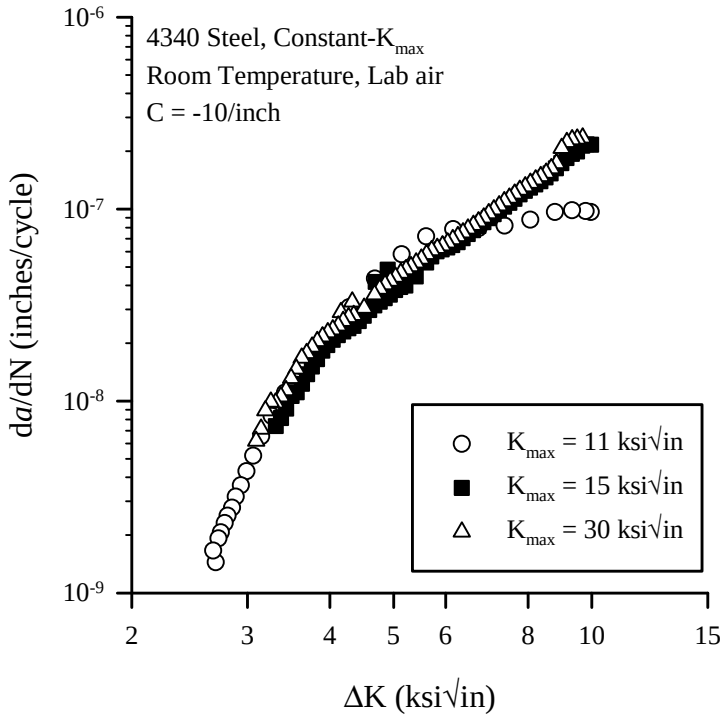

Figure 10. Constant-K_{max} fatigue crack growth data for 4340 steel.

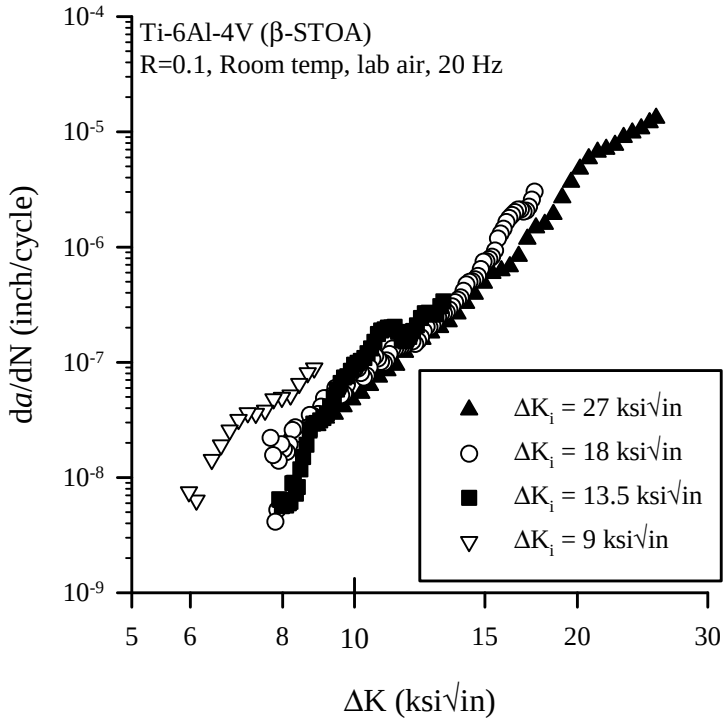

Figure 11. Constant-R = 0.1 fatigue crack growth data for Ti-6Al-4V (β-STOA).

Constant-R = 0.1 test data for Ti-6Al-4V are shown in Figure 11 for initial ΔK values of ΔK_i = 27 ksi√in, 18 ksi√in, 13.5 ksi√in, and 9 ksi√in. With the exception of the data set initiated at ΔK_i = 9 ksi√in, these data are generally in good agreement. However, there appears to be a significant degree of scatter or randomness associated with these data. For example, the crack growth rates for the ΔK_i = 13.5 ksi√in are initially greater than for the tests started at higher ΔK values. As ΔK decreased below 9 ksi√in, the crack growth rates were lower than for tests at higher ΔK_i. This behavior is not be expected if load history effects were the primary cause of differences in these data. A significantly lower ΔK_{th} is observed for the test results corresponding to the lowest ΔK_i value (ΔK_i = 9 ksi√in). However, during this test the crack deviated out of plane by nearly 10^o, and crack length measurements on each side of the specimen indicated that the crack growth was significantly slower on one side relative to the other (crack front did not remain straight).

A highly tortuous crack path was observed during all tests, with typical asperity dimensions similar to the average grain diameter (1 mm). The titanium specimens used were 0.5 inches (12.7 mm) thick, or approximately 13 grain diameters. Considering that the entire crack front would likely be contained within such a limited number of grains at any given time, it is not unreasonable to believe that the variability or randomness observed in the data of Figure 11 are due to microstructural effects. Due to concerns that microstructural effects are significant, this alloy is a poor choice for a study on load history effects.

Constant-R = 0.5 data for titanium are shown in Figure 12. Here, the crack growth curve is comprised of results from two tests, a decreasing-ΔK test initiated at ΔK_i = 5.5 ksi√in and an increasing-ΔK test initiated at ΔK_i = 4.0 ksi√in. Considering that these data appear to contain a significant degree of randomness (similar to the R = 0.1 results), good agreement is seen between these data where values of ΔK coincide (4.0 ksi√in < ΔK < 5.5 ksi√in).

Constant-R = 0.7 data for titanium are shown in Figure 13. Here, the crack growth curve is comprised of results from three tests, a decreasing-ΔK test initiated at ΔK_i = 4.5 ksi√in and two increasing-ΔK tests initiated at ΔK_i = 4.0 ksi√in and 11.0 ksi√in. The variability seen in Figures 11 and 12 are also observed in Figure 13, especially near the fatigue crack growth threshold. Considering the inherent variability associated with this material, the data of Figure 13 are in good agreement.

Constant-K_{max} fatigue crack growth data for titanium are plotted in Figure 14 for three K_{max} levels; K_{max} = 40 ksi√in, 20 ksi√in, and 10 ksi√in. Higher crack growth rates, d*a*/dN, and lower crack growth thresholds, ΔK_{th}, are observed with increasing K_{max}. Here, the threshold decreases from approximately ΔK_{th} = 3.8 ksi√in to 2.5 ksi√in as K_{max} increases from K_{max} = 10 ksi√in to 40 ksi√in, respectively, a 34% reduction in ΔK_{th}. Although no additional constant-K_{max} testing was performed, further reduction in ΔK_{th} is expected to occur for K_{max} values greater than 40 ksi√in.

AZ91E Magnesium

AZ91E Magnesium was provided in cast plates approximately 14 inches square and 0.5 inches thick. Compact tension specimens (W = 2 inches, B = 0.25 inches) were machined from these plates with the specimen sides at least 0.5 inches from the plate edges to avoid any microstructural gradient that may have been created during processing. Additionally, the outer surfaces of the plate were milled down approximately 1/8 inch (creating a 0.25 inch thick specimen from a 0.5 inch thick plate) to avoid any microstructural gradient that may exist near the plate surface.

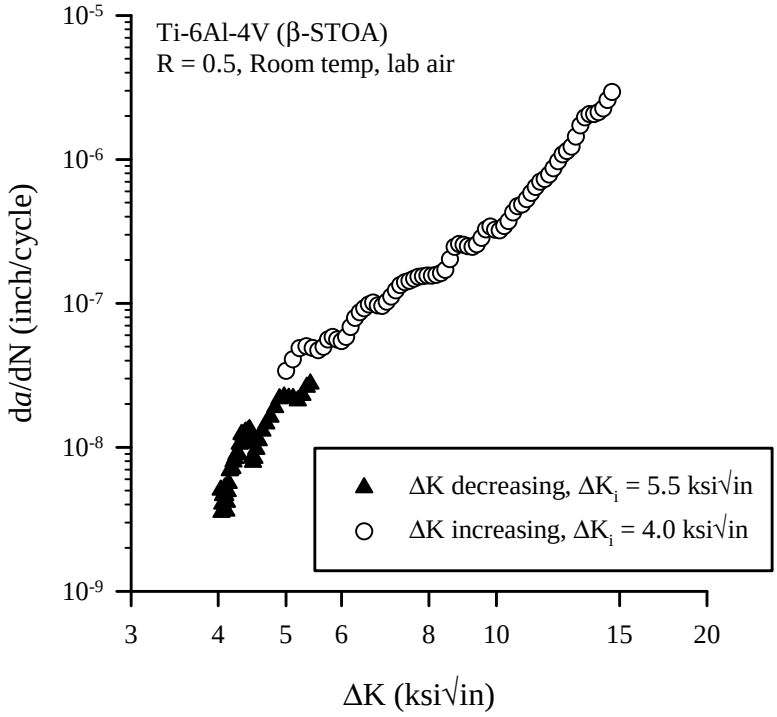

Figure 12. Constant-R = 0.5 fatigue crack growth data for Ti-6Al-4V (β-STOA).

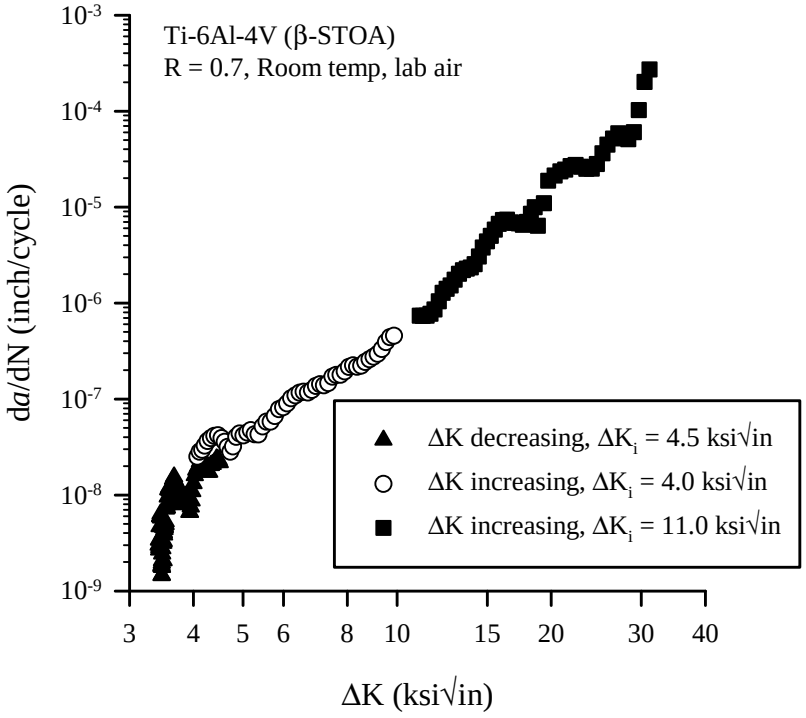

Figure 13. Constant-R = 0.7 fatigue crack growth data for Ti-6Al-4V (β-STOA).

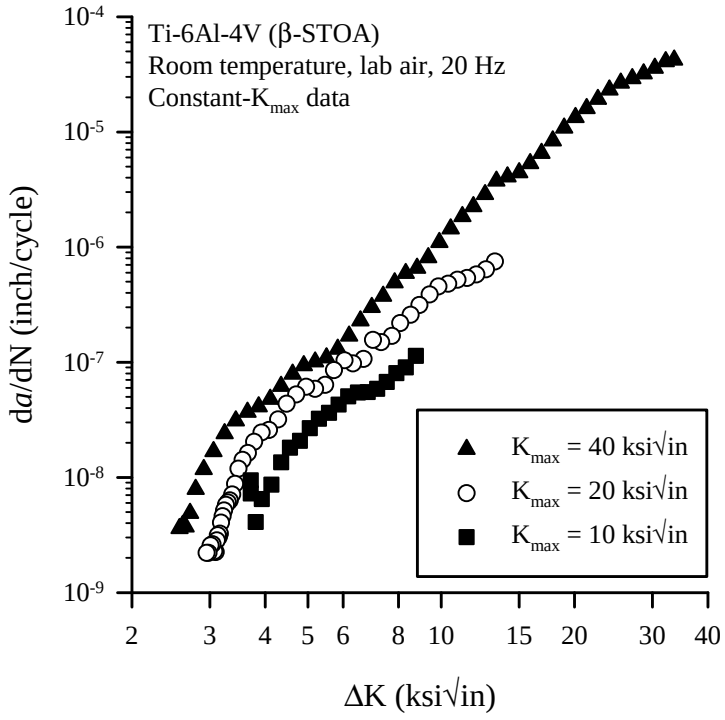

Figure 14. Constant-K_{max} fatigue crack growth data for Ti-6Al-4V (β-STOA).

Constant-R = 0.1 fatigue crack growth data for magnesium are plotted in Figure 15. Two increasing-ΔK tests (ΔK_i = 4.8 ksi√in and 2.8 ksi√in) and two decreasing-ΔK tests (ΔK_i = 4.5 ksi√in and 2.0 ksi√in) are shown. All of these results are in excellent agreement suggesting that the fatigue crack growth rate data is not sensitive to load history. These data suggest that the R = 0.1 threshold is approximately ΔK_{th} = 1.65 ksi√in. The high ΔK data show that crack growth rates rapidly increase with increasing ΔK until specimen failure occurs at approximately ΔK = 14 ksi√in (K_{max} = 15.5 ksi√in). Although not a standard fracture toughness test, this provides an unofficial estimate of the effective cyclic fracture toughness.

Due to the excellent agreement observed in the constant-R = 0.1 data (see Figure 15), load history is not expected to be an issue at higher R. Constant-R = 0.7 fatigue crack growth data for magnesium are plotted in Figure 16. Results for two tests are shown (one ΔK increasing and one ΔK decreasing). The fatigue crack growth rate data for these tests are in excellent agreement. The results shown in Figure 16 indicate that the R = 0.7 threshold for this material is approximately ΔK_{th} = 1.02 ksi√in. The higher ΔK results show rapidly increasing d*a*/dN with increasing ΔK until specimen failure occurs at ΔK = 4.4 ksi√in (K_{max} = 14.7 ksi√in), which is similar to the non-standard effective toughness value obtained from the R = 0.1 results.

Constant-K_{max} fatigue crack growth data for magnesium are shown in Figure 17 for K_{max} levels of 10 ksi√in and 5 ksi√in. As the constant-R = 0.1 and constant-R = 0.7 results indicate the toughness of this alloy to be approximately K_c = 15 ksi√in, no effort was made to perform a test at higher K_{max} levels. The fatigue crack growth threshold was observed to decrease from approximately ΔK_{th} = 0.98 ksi√in to ΔK_{th} = 0.72 ksi√in as the K_{max} value increased from 5 ksi√in to 10 ksi√in, respectively, a 27% reduction. Considering that K_{max} = 10 ksi√in is likely greater than 65% of the material toughness, this observation suggests that fatigue crack growth rates are elevated at high K_{max} values.

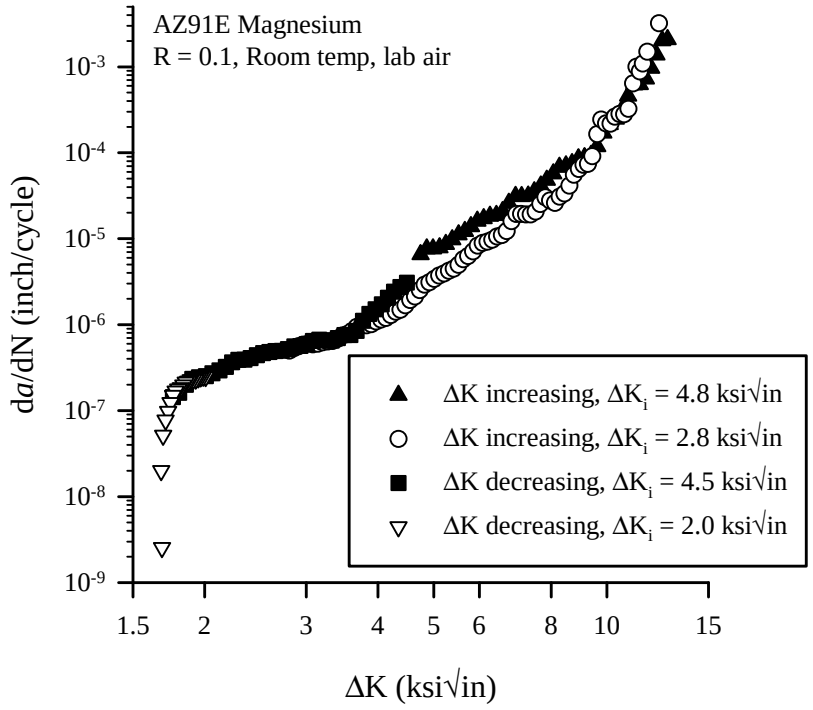

Figure 15. Constant-R = 0.1 fatigue crack growth data for AZ91E Magnesium.

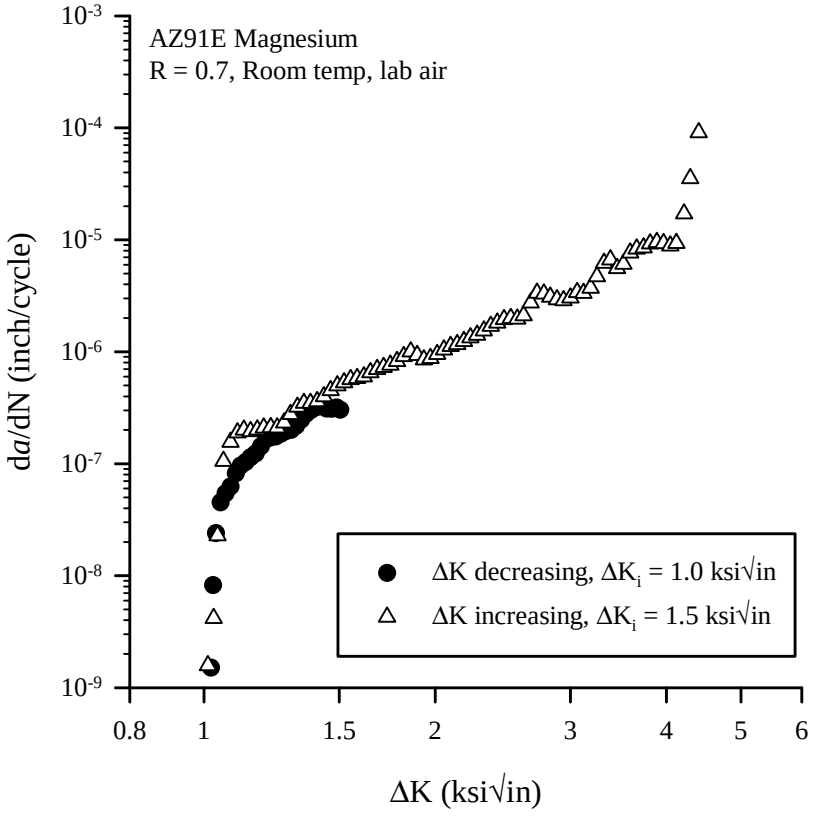

Figure 16. Constant-R = 0.7 fatigue crack growth data for AZ91E Magnesium.

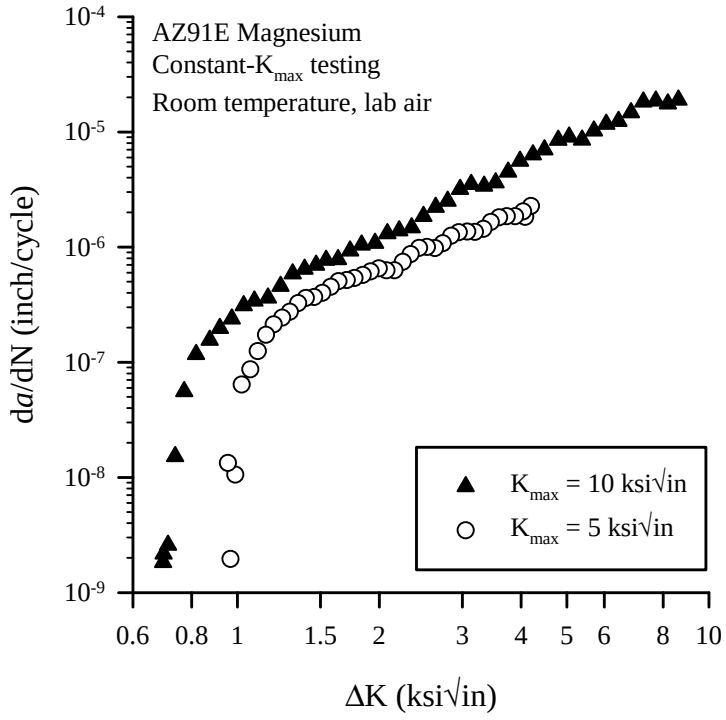

Figure 17. Constant-K_{max} fatigue crack growth data for AZ91E Magnesium.

Discussion of Results

The objectives of this study were to (1) generate fatigue crack growth data needed for damage tolerance life predictions for rotorcraft materials and (2) determine if the ASTM standard method for fatigue crack growth testing was affected by load history. Originally, tests were planned to evaluate an alternate test method where specimens were pre-cracked under compressive applied loading, however, this portion of the test program was abandoned after preliminary results revealed problems with this compressive pre-cracking test method (see Appendix).

The fatigue crack growth results were presented in Figures 3-17. For standard ΔK-reduction tests on aluminum alloy 7050 for R = 0.1, a slight increase in crack growth threshold (ΔK_{th}) was observed with initial ΔK value (ΔK_i) as shown in Figure 18. Crack growth threshold (open circular symbols) and the crack growth rate (d*a*/dN) corresponding to the start of the test (solid triangular symbols) are plotted against initial ΔK. If all of these tests were unaffected by load history, then ΔK_{th} should be independent of ΔK_i (horizontal line in Figure 18), however, there does appear to be a subtle trend for increasing ΔK_{th} with increasing ΔK_i. Considering that the extreme values of ΔK_{th} do not correspond to the extreme values of ΔK_i, it seems that there is an element of scatter or unexplained variation in these data. It is possible that an uncontrolled variable, such as humidity (ref. 7), is responsible for this variation and potentially has a greater influence on ΔK_{th} than load history (ΔK_i).

The initial crack growth rates are considered of interest because ASTM Standard E647, Section 8.6 does not recommend starting ΔK-reduction tests at crack growth rates greater than 4×10^{-7} inches/cycle (10^{-8} m/cycle). This upper bound on initial crack growth rate is shown on the right side of Figure 18 as a horizontal dashed line. Tests started at ΔK_i = 9.0 ksi√in and 7.2 ksi√in violate this recommendation

(because those data are above the horizontal dashed line) while the tests started at ΔK_i = 4.5 ksi√in and 3.15 ksi√in satisfy this recommendation. Note that these tests were intentionally performed in violation of ASTM Standard E647, Section 8.6, to exacerbate potential load history effects. Considering that the high ΔK_i data fails to meet all recommendations of ASTM E647, no clear trend in ΔK_{th}, as a function of ΔK_i, is obvious, although, more results are needed to characterize such a small influence.

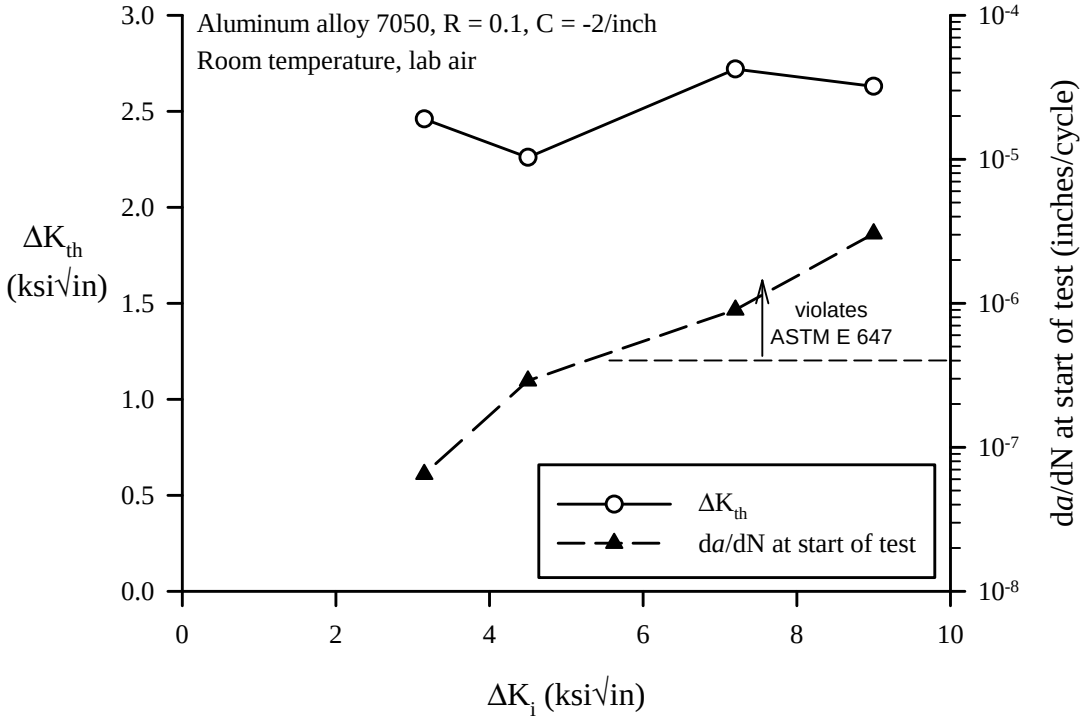

Figure 18. Plot of critical parameters for R = 0.1 ΔK-reduction tests on aluminum alloy 7050.

Similar analysis of the titanium R = 0.1 data is difficult due to the significant variation in the crack growth data. Presumably, this variation is due to the large grain size of this alloy. Considering that the average grain diameter is approximately 1 mm (0.04 inches), a crack front (nominal specimen thickness = 0.5 inches) may be contained within as few as 13 grains, which may explain the scatter in the data. There is excellent agreement between all sets of R = 0.1 data, with the exception of the test started at the lowest ΔK_i (ΔK_i = 9 ksi√in), which produced a threshold of approximately ΔK_{th} = 6 ksi√in, which was nearly 25% lower than the other tests (ΔK_{th} = 8 ksi√in). No observations were made to explain this observation; further study is needed to determine what conditions, if any, that R = 0.1 crack growth is possible for ΔK < 6 ksi√in.

No load history effects, here considered to be variation in ΔK_{th} as a function of ΔK_i, were noted for the other alloys (4340 steel, Ti-6Al-4V, and AZ91E magnesium), so no further scrutiny was given to these alloys. Factors not considered in this study, such as microstructural effects and environment (ref. 7), or K_{max} effects (ref. 14), appeared to have a greater influence on the crack growth threshold (ΔK_{th}) than load history, at least for the alloys and test conditions examined.

Summary

The results of a fatigue crack growth study, conducted on commonly-used rotorcraft alloys, have been presented. Due to concerns in the fracture mechanics community regarding load history effects during standard ΔK-reduction fatigue crack growth testing, special attention was given to the possibility of load history effects; defined as crack growth results that are artificially affected by details of the test procedure. A series of tests were performed, with emphasis on R = 0.1 (where load history effects are believed to be most significant), with different initial ΔK values (ΔK_i). The results presented in this document revealed almost no evidence of load history for two alloys (AZ91E magnesium and 4340 steel). For the two other alloys (7050 aluminum and Ti-6Al-4V (β-STOA)) subtle differences in crack growth threshold (ΔK_{th}) for different ΔK_i were observed, but no obvious trends were found, possibly suggesting that other variables (e.g., microstructure variations or variable humidity levels) could be responsible for this behavior.

An alternate crack growth test method, called compression precracking, where cracks are initiated in standard compact specimen by cyclically applied compressive loads, was also evaluated. Analysis of the results showed little or no apparent load history effects where ASTM Standard E647, and all recommendations, was strictly followed. However, the compression precracking test method was shown to produce load history effects, resulting from tensile compressive stresses imparted during compressive loading, which significantly affected the subsequent near-threshold crack growth rate data. Based on the findings presented in this paper, no load history problems were found when the standard crack growth test procedure (ASTM E647) was strictly followed.

References

(1) Palmgren, A., "Ball and Roller Bearing Engineer," translated by A. Palmgren and B. Ruley, SKF Industries, Inc., Philadelphia, 1945, pp. 82-83.

(2) Miner, M.A., "Cumulative Damage in Fatigue," *Journal of Applied Mechanics*, ASME, Vol. 12, Sept. 1945.

(3) Tritsch, D.E., Schneider, G.J., Chamberlain, G., and Lincoln, J.W., "Damage Tolerance Assessment of the HH-53 Helicopter," Proceedings of the 46th Annual Forum of the American Helicopter Society, Washington D.C., 1990.

(4) Everett, R.A., Jr. "Crack-Growth Characteristics of Fixed- and Rotary-Wing Aircraft," 6th Joint FAA/DoD/NASA Aging Aircraft Conference, San Francisco, CA, Sept.16-19, 2002.

(5) ASTM E 647– 00, "Standard Test Method for Measurement of Fatigue Crack Growth Rates," Annual Book of ASTM Standards, Section 8, Vol. 03.01.

(6) Pippan, R., Stuwe, H.P., and Golos, K., "A Comparison of Different Methods to Determine the Threshold of Fatigue Crack Propagation," Fatigue, Vol. 16, 1994.

(7) Bush, R.W., Donald, J.K., and Bucci, R.J., "Pitfalls to Avoid in Threshold Testing and its Interpretation," *Fatigue Crack Growth Thresholds, Endurance Limits, and Design, ASTM STP 1372*, J.C. Newman, Jr. and R.S. Piascik, Eds., American Society for Testing and Materials, West Conshohocken, PA, 2000, pp. 269-284.

(8) Suresh, S., "Crack Initiation in Cyclic Compression and its Applications," *Engineering Fracture Mechanics*, Vol. 21, 1985, pp. 453-463.

(9) Forth, S.C., Newman, J.C., Jr., and Forman, R.G., "On Generating Fatigue Crack Growth Thresholds," *International Journal of Fatigue*, Vol. 25, 2003.

(10) James, M.A., Forth S.C., and Newman, J.A., "Load History Effects Resulting from Compression Precracking," Fatigue and Fracture Mechanics: 34th Volume, ASTM STP 1461, S. Daniewicz, J.C. Newman, Jr., and H. Schwalbe, Eds., American Society for Testing and Materials, West Conshohocken, PA, 2004, pp. 43-59.

(11) Newman, J.C., Jr., "Analyses of Fatigue Crack Growth and Closure Near Threshold Conditions for Large-Crack Behavior," *Fatigue Crack Growth Thresholds, Endurance Limits, and Design, ASTM STP 1372*, J.C. Newman, Jr. and R.S. Piascik, Eds., American Society for Testing and Materials, West Conshohocken, PA, 2000, pp. 227-251.

(12) Forth, S.C., James, M.A., Newman, J.A., Everett, R.A., Jr., and Johnston, W.M., "Mechanical Data for Use in Damage Tolerance Analyses," NASA/TM-2004-213503.

(13) Sheldon, J.W., Bain, K.R., and Donald, J.K., "Investigation of the Effects of Shed-Rate, Initial K_{max}, and Geometric Constraint on ΔK_{th} in Ti-6Al-4V at Room Temperature," *International Journal of Fatigue*, Vol. 21, 1999, pp. 733-741.

(14) Newman, J.A., Riddell, W.T., and Piascik, R.S., "Effects of K_{max} on Fatigue Crack Growth Threshold in Aluminum Alloys," Fatigue Crack Growth Thresholds, Endurance Limits, and Design, ASTM STP 1372, J.C. Newman, Jr. and R.S. Piascik, Eds., American Society for Testing and Materials, 2000, West Conshohocken, PA, pp. 63-77.

Appendix – Compression Precracking Results

Compression precracking tests were conducted by initiating fatigue cracks under cyclic compressive loads (refs. 9, 10, 12). A small tensile zone exists near the crack starter notch, which permits crack initiation, but without leaving large-scale plasticity in the crack wake. Without a significant amount of crack wake plasticity, crack growth testing can be started at low ΔK values (near the fatigue crack growth threshold). However, recent results have shown that compression precracking introduces significant residual tensile stresses that affect fatigue crack growth rates during subsequent testing (ref. 10). Constant-ΔK tests were used to evaluate the extent of the CPC-induced residual stress zone. Under constant-ΔK conditions crack growth results plotted as crack length versus cycle count should show a constant slope if steady-state conditions exist.[3] After compression precracking, the tensile residual stress is known to decrease as the crack propagates, such that the effective load ratio decreases from an artificially high value (depending on the severity of the compression precracking) to asymptotically approach the applied load ratio.

The results for a typical CPC test are shown in Figures A1 through A3. For this example, an aluminum 7050 CT specimen (W = 2 inches, B = 0.25 inches) was subjected to compression precracking at P_{min} = -108 lbf and P_{max} = -5.4 lbf, followed by tensile loading at P_{max} = 175 lbf and R = 0.1. The crack-length-versus-cycle-count data during the compressive precracking are shown in Figure A1. Note that crack length values shown in Figure A1 are relative to the tip of the crack-starter notch, which has a length of 0.396 inches relative to the axis of applied loading (pin-hole center line). Initially, a high crack growth rate (slope of the curve) is observed; nearly 0.018 inches of crack growth occurs in the first 1,000 cycles. As the crack propagates out to approximately 0.030 inches, a significant reduction in crack growth rate occurs. CPC is stopped after 16,000 cycles and approximately 0.037 inches of crack growth. Only 4,000 cycles (25% of the total) is required to produce approximately 0.028 inches of crack growth (75% of the total).

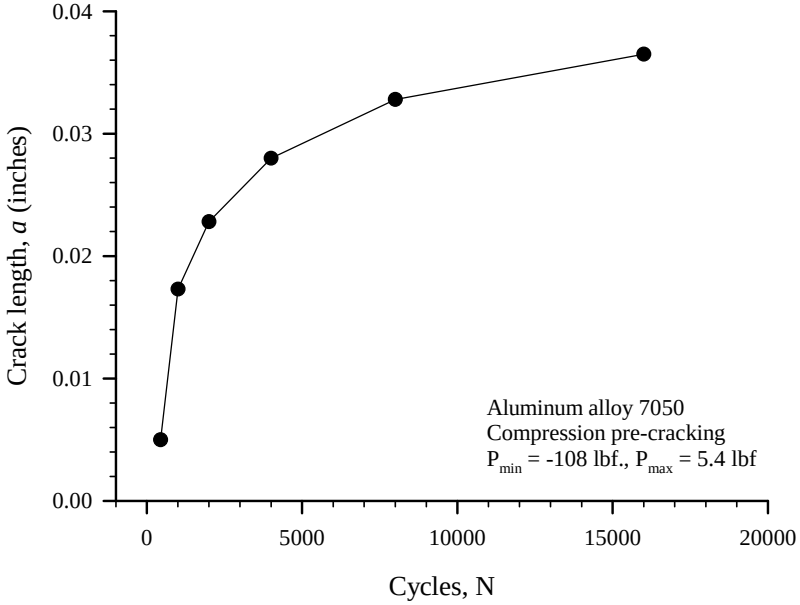

Figure A1. Typical plot of crack-length-versus-cycle-count data during CPC testing.

[3] The slope of the crack-length-versus-cycle-count curve is the crack growth rate, d*a*/dN.

Following the compression precracking, a constant-load test was performed at P_{max} = 174 lbf and R = 0.1. Crack-length-versus-cycle-count data for this test are shown in Figure A2. As the crack propagates under constant-load conditions, the crack-tip stress intensity factor gradually increases resulting in a gradual increase in d*a*/dN. The corresponding crack growth rate data for this test are shown in Figure A3.

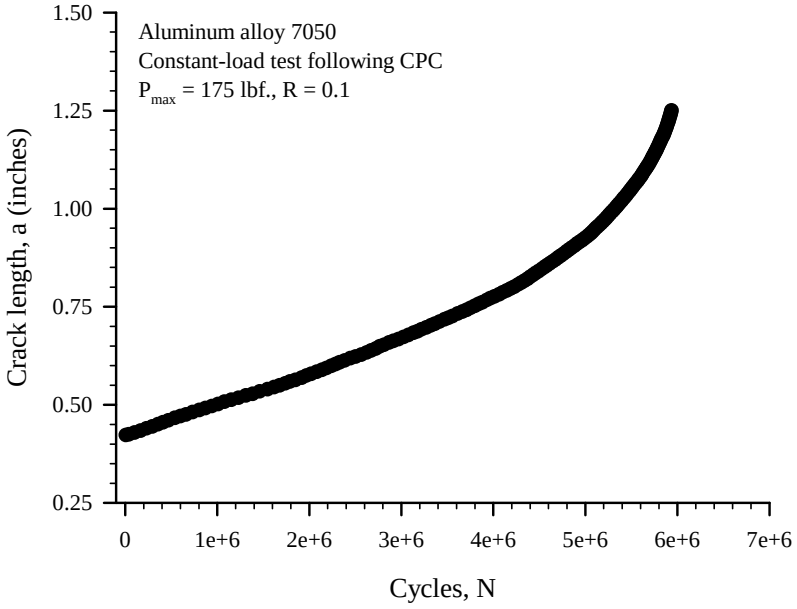

Figure A2. Plot of crack-length-versus-cycle-count data for constant-load testing following CPC testing.

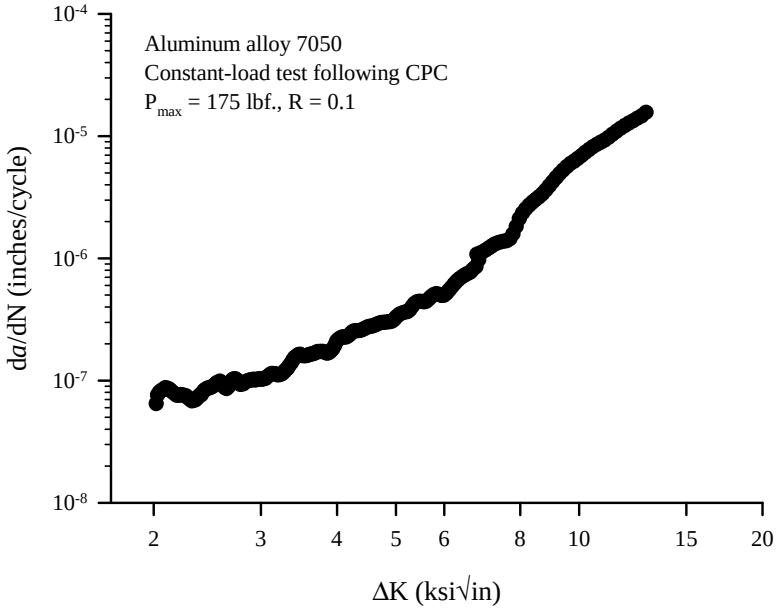

Figure A3. Plot of crack growth rate data for constant-load testing following CPC testing.

The CPC test method was proposed as an alternate test method that would be free of load history tests which may affect standard test data. However, recent analytical and experimental results have suggested that compression loading at the crack starter notch produces significant tensile residual stresses that affect subsequent crack growth (ref. 10). Resolving this issue by comparing standard test data with CPC test data has not proved useful as is illustrated in the following example.

In Figure A4, the CPC crack growth data of Figure A3 are plotted with constant-R = 0.1 ΔK-reduction data from Figure 3 for comparison. Here, two standard R = 0.1 curves are shown corresponding to initial ΔK values of ΔK_i = 4.5 ksi√in and 9.0 ksi√in (open triangular symbols and open square symbols, respectively). Note that each of the standard tests is in good agreement with the CPC test at higher ΔK values corresponding to the initiation of the ΔK-reduction tests. At lower ΔK values, especially near the crack growth thresholds, the standard test data does not agree well with the CPC test. Considering that the CPC test was designed to avoid load history effects that may occur during standard ΔK-reduction testing, and that such load history effects presumably would grow larger as the test progressed (greater ΔK reduction), it seems reasonable to suspect that (1) the two sets of standard data are affected by some load history effect and (2) the CPC test method may be avoiding, or at least be less affected by, this load history.

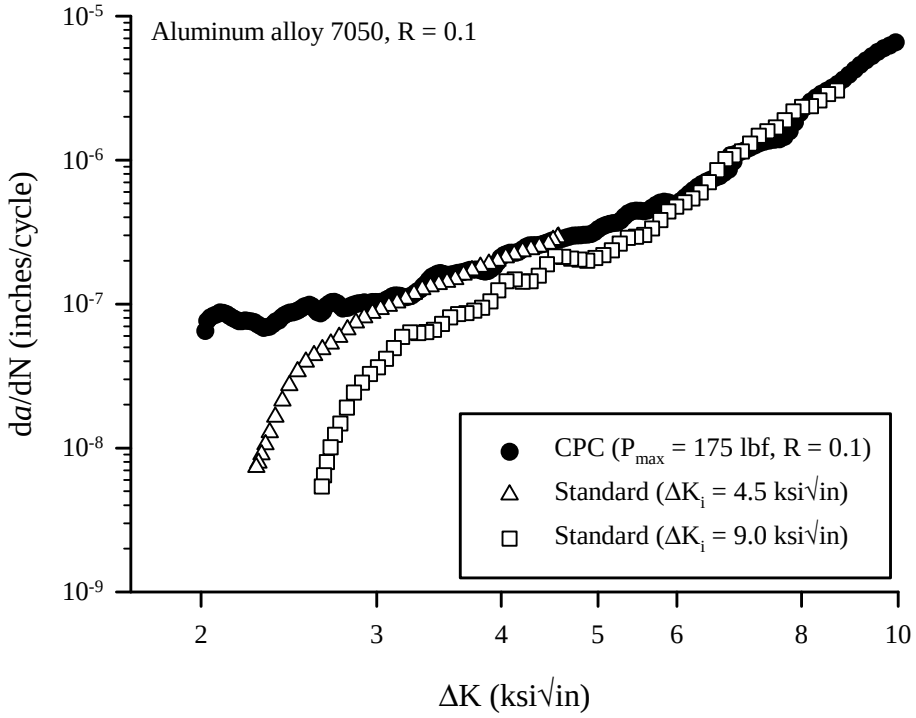

Figure A4. Comparison of CPC and standard low-R test results.

In Figure A5, these same CPC test data are compared with the constant-K_{max} test data (5 ksi√in and 10 ksi√in) of Figure 6. Each constant-K_{max} test was started at R = 0.1 test conditions (ΔK_i = 9 ksi√in and 4.5 ksi√in for constant-K_{max} values of 5 ksi√in and 10 ksi√in, respectively), and it should be noted that the CPC test results are in good agreement with the constant-K_{max} test data at the ΔK values corresponding to initiation. Considering that constant-K_{max} tests produce very high values of R near the crack growth threshold it is surprising that the CPC test data is found to be in good agreement with constant-K_{max} data near ΔK = 2 ksi√in. For this condition the constant-K_{max} test is operating at R = 0.8, where crack closure

is widely believed to be a non-factor (ref. 14); however, since the CPC test uses a standard long-crack test specimen at R = 0.1 where some crack closure (not related to load history) would be expected. Considering that a previous study (ref. 10) has shown that CPC testing produces a large tensile residual stress field near the crack-starter notch, and that the magnitude of residual stress decays as the crack propagates, it seems reasonable to suspect that the CPC test agrees at low ΔK due to high residual stresses effectively creating high R crack-tip conditions, and, at higher R these sets of data agree where they should after the magnitude of residual stress has sufficiently decayed. These preliminary results indicate that further study is needed to determine if the CPC test method produces usable fatigue crack growth data.

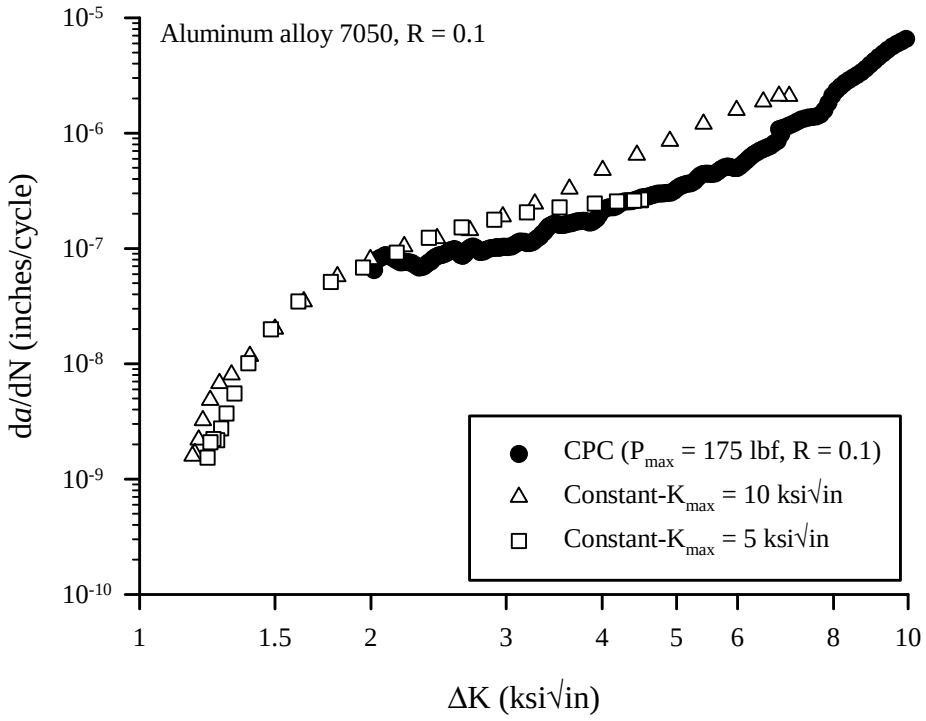

Figure A5. Comparison of CPC and constant-K_{max} test results.

REPORT DOCUMENTATION PAGE

Form Approved
OMB No. 0704-0188

1. REPORT DATE *(DD-MM-YYYY)*	2. REPORT TYPE	3. DATES COVERED *(From - To)*
01- 07 - 2008	Technical Memorandum	

4. TITLE AND SUBTITLE
Fatigue Crack Growth Threshold Testing of Metallic Rotorcraft materials

5a. CONTRACT NUMBER

5b. GRANT NUMBER

5c. PROGRAM ELEMENT NUMBER

6. AUTHOR(S)
Newman, John A.; James, Mark A.; Johnston, William M.; and Le, Dy D.

5d. PROJECT NUMBER

5e. TASK NUMBER

5f. WORK UNIT NUMBER
698259.02.07.07.03.02

7. PERFORMING ORGANIZATION NAME(S) AND ADDRESS(ES)
NASA Langley Research Center
Hampton, VA 23681-0001

U.S. Army Research Laboratory
Vehicle Technology Directorate
NASA Langley Research Center
Hampton, VA 23681-2199

8. PERFORMING ORGANIZATION REPORT NUMBER
L-19489

9. SPONSORING/MONITORING AGENCY NAME(S) AND ADDRESS(ES)
National Aeronautics and Space Administration
Washington, DC 20546-0001 and
U.S. Army Research Laboratory
Adelphi, MD 20783-1145

10. SPONSOR/MONITOR'S ACRONYM(S)
NASA

11. SPONSOR/MONITOR'S REPORT NUMBER(S)
NASA/TM-2008-215331 ARL-TR-4472

12. DISTRIBUTION/AVAILABILITY STATEMENT
Unclassified - Unlimited
Subject Category 26
Availability: NASA CASI (301) 621-0390

13. SUPPLEMENTARY NOTES
An electronic version can be found at http://ntrs.nasa.gov

14. ABSTRACT

Results are presented for a program to determine the near-threshold fatigue crack growth behavior appropriate for metallic rotorcraft alloys. Four alloys, all commonly used in the manufacture of rotorcraft, were selected for study: Aluminum alloy 7050, 4340 steel, AZ91E Magnesium, and Titanium alloy Ti-6Al-4V (?-STOA). The Federal Aviation Administration (FAA) sponsored this research to advance efforts to incorporate damage tolerance design and analysis as requirements for rotorcraft certification. Rotocraft components are subjected to high-cycle fatigue and are typically subjected to higher stresses and more stress cycles per flight hour than fixed-wing aircraft components. Fatigue lives of rotorcraft components are generally spent initiating small fatigue cracks that propagate slowly under near-threshold crack-tip loading conditions. For these components, the fatigue life is very sensitive to the near-threshold characteristics of the material.

15. SUBJECT TERMS
Fatigue crack growth; Load reduction testing; Rotocraft; Threshold

16. SECURITY CLASSIFICATION OF:			17. LIMITATION OF ABSTRACT	18. NUMBER OF PAGES	19a. NAME OF RESPONSIBLE PERSON
a. REPORT	b. ABSTRACT	c. THIS PAGE			STI Help Desk (email: help@sti.nasa.gov)
					19b. TELEPHONE NUMBER *(Include area code)*
U	U	U	UU	27	(301) 621-0390